Optical dipole model for photodetection in the near field

R. C. Davis

Brigham Young University, Provo, Utah 84602

C. C. Williams

University of Utah, Salt Lake City, Utah 84112

Received September 11, 2000; accepted October 10, 2000; revised manuscript received November 16, 2000

Near-field photodetection optical microscopy (NPOM) is a scanning probe technique that has been developed to perform nanometer-scale optical intensity mapping and spectroscopy. In NPOM a nanometer-scale photodiode detector absorbs power directly as it is scanned in the near field of an illuminated sample surface. A model of photodetection in the near and intermediate fields is presented. A brief review of far-field absorption is given for comparison. Far-field absorption measurements measure the imaginary part of the polarizability to first order. In contrast, photodetection in the near field measures the real part of the polarizability. Other aspects of near-field photodetection are also examined, including contrast mechanisms and lateral resolution. NPOM measurements performed on isolated 300-nm spheres show good agreement with the theory. © 2001 Optical Society of America

OCIS codes: 180.5810, 180.0180, 240.0240.

1. INTRODUCTION

Optical measurements on the nanometer scale are now possible with optical scanning probe techniques. Among the promising capabilities of these near-field optical microscopies is optical spectroscopy, in particular its application to generic molecular identification on the nanometer scale. An understanding of the physical optics in the near field is necessary to reliably interpret these measurements and make possible their use in a broad range of applications.

Several scanning probe near-field optical techniques have now been developed. Near-field scanning optical microscopy (NSOM) is a technique based on the collection or the transmission of light through a subwavelength aperture scanned near a surface.[1,2] Nanometer-scale optical microscopy has also been performed without an aperture using techniques based on scattering from or field enhancement by an atomic force microscope tip near the sample.[3,4]

Near-field photodetection optical microscopy (NPOM)[5–14] is a fundamentally different approach from near-field optical microscopy that has been developed to perform nanometer-scale optical intensity mapping and spectroscopy. In NPOM a photodetector of subwavelength dimensions is brought into the optical near field of an illuminated surface (conducting or nonconducting), where it can directly absorb optical power [Fig. 1(a)]. A noncontact atomic force microscope can be used for height control. As the photodetector is raster scanned across the surface, the photocurrent signal is recorded to create a two-dimensional image of the optical intensity distribution [Fig. 1(b)]. Recently, the first nanometer-scale photodiode probes for NPOM have been fabricated.[9,12] The probes have an optically sensitive area of 100 nm $\times$ 100 nm and a detection sensitivity of $150\,fW/\sqrt{\mathrm{Hz}}$. Near-field photodetection optical microscopy and spectroscopy have been demonstrated with the use of these high-resolution probes.[9,12,13]

The propagation of light through nanometer-scale structures has been studied numerically for the specific geometries of both aperture-based and photon tunneling NSOM.[15–17] A general treatment of transmission mode NSOM employing a dipole model has been used to study contrast mechanisms in allowed and forbidden light imaging modes.[18]

Here we present a dipole model of photodetection that we have developed for NPOM. The effect of the real and the imaginary part of the sample polarizability on the photocurrent is examined. This information is specifically needed for the interpretation of near-field photodetection spectroscopy, a technique similar to far-field absorption spectroscopy (spectrophotometry).[13] It has not yet been established whether near-field photodetection spectroscopy and absorption spectroscopy measurements are equivalent. The dipole model presented here will allow us to address this question. Other aspects of near-field photodetection are also examined, including contrast mechanisms and lateral resolution.

The outline of the paper is as follows. A brief review of the physical basis of far-field absorption and scattering will be given in Section 2 to provide a background context for photodetection in the near field. An analysis of near-field photodetection will then follow. In Section 3, a two-dipole theory of near-field photodetection will be presented. The effects of sample polarizability, imaging contrast mechanisms, and spatial resolution will be examined. In Section 4, NPOM imaging in the intermediate field will be considered.

0740-3232/2001/071543-09$15.00

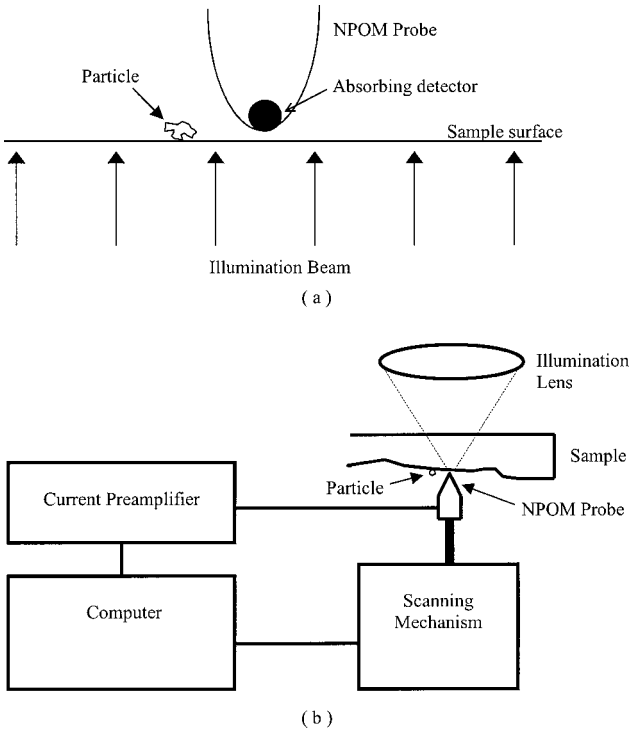

Fig. 1. Near-field photodetection optical microscopy (NPOM). (a) An absorbing detector is brought into the near field of an illuminated sample surface. (b) The probe is rastor scanned and the photocurrent is recorded to generate a two-dimensional image of the optical intensity distribution.

2. EXTINCTION IN THE FAR FIELD

In standard photometric measurement (far field), light is scattered and absorbed by the sample. The detector collects the light that is transmitted through the sample. This transmitted light is the incident light less the scattered and the absorbed light. The removal of power from the beam by scattering and absorption is called extinction. In this section, coherent extinction by a single particle that is small compared with the wavelength will be examined.

A particle, illuminated by a monochromatic plane electromagnetic wave $\mathbf{E}_i$, $\mathbf{H}_i$ generates a scattered wave $\mathbf{E}_s$, $\mathbf{H}_s$ (see Fig. 2):

$$\mathbf{E}_i = \mathbf{E}_0 \exp(i\mathbf{k} \cdot \mathbf{r} - i\omega t),$$

$$\mathbf{H}_i = \sqrt{\epsilon_0/\mu_0}\mathbf{k} \times \mathbf{E}_i . \tag{1}$$

The surrounding electric and magnetic fields are the sum of the incident and scattered waves. It is useful to consider three different regions: the near field, when $kr \ll 1$; the far field, when $kr \gg 1$; and the intermediate field, when kr is of order 1.

We will consider first the far field ($kr \gg 1$), where absorption spectroscopy measurements have traditionally been performed. The problem of extinction in far-field measurements is treated in the book by van de Hulst[19] and more recently in the book by Bohren and Huffman.[20] Our notation more closely follows that of Bohren and Huffman. Coherent extinction by small particles in the focal volume of a lens has been treated by Pettit and Peterson.[21,22]

The power absorbed by the particle, W_a, is calculated by integrating the normal component of the Poynting vector $\mathbf{S}$ over the surface of an imaginary sphere, σ, centered on the particle (see Fig. 3):

$$W_a = -\int_\sigma \mathbf{S} \cdot \mathrm{d}\mathbf{A}. \tag{2}$$

Note that W_a is always positive for a passive absorbing particle. The time-averaged Poynting vector $\mathbf{S}$ can be broken into three components as follows:

$$\mathbf{S} = \mathbf{S}_i + \mathbf{S}_{\text{ext}} + \mathbf{S}_s . \tag{3}$$

$\mathbf{S}_i$, $\mathbf{S}_{\text{ext}}$, and $\mathbf{S}_s$ are the incident, extinction, and scattering components of the Poynting vector:

$$\mathbf{S}_i = \tfrac{1}{2}\,\mathrm{Re}(\mathbf{E}_i \times \mathbf{H}_i^*),$$

$$\mathbf{S}_{\text{ext}} = \tfrac{1}{2}\,\mathrm{Re}[(\mathbf{E}_i \times \mathbf{H}_s^*) + (\mathbf{E}_s \times \mathbf{H}_i^*)],$$

$$\mathbf{S}_s = \tfrac{1}{2}\,\mathrm{Re}(\mathbf{E}_s \times \mathbf{H}_s^*). \tag{4}$$

The absorbed (W_a), the scattered (W_s), and the extinguished (W_{ext}) power can be calculated as follows:

$$W_a = -\int_\sigma \mathbf{S} \cdot \mathrm{d}\mathbf{A},$$

$$W_s = \int_\sigma \mathbf{S}_s \cdot \mathrm{d}\mathbf{A},$$

$$W_{\text{ext}} = -\int_\sigma \mathbf{S}_{\text{ext}} \cdot \mathrm{d}\mathbf{A} \tag{5}$$

(note the minus sign).

The net power flux of the incident beam across the surface σ is zero, therefore the following simple relation holds exactly:

$$W_{\text{ext}} = W_a + W_s . \tag{6}$$

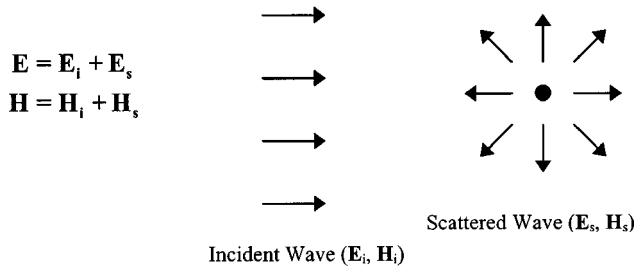

Fig. 2. Incident and scattered waves in the vicinity of an illuminated particle. Arrows indicate the direction of propagation of the waves.

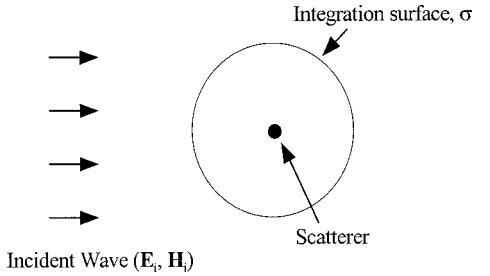

Fig. 3. Absorption and scattering by a particle.

The mathematical expressions for the extinction terms given in Eqs. (4) and (5) are consistent with the physical definition given in the first paragraph of this section, i.e., the power extinguished from the incident beam is equal to the sum of the power absorbed and scattered out of the beam by the particle.

A. Power into the Detector

The far-field absorption measurement is set up as follows. A small detector of area D is placed on the right-hand side of the imaginary surface σ in the forward-scattering direction (see Fig. 4). The power into the detector is given by

$$W_d = \int_D \mathbf{S} \cdot d\mathbf{A} = \int_D \mathbf{S}_i \cdot d\mathbf{A} + \int_D \mathbf{S}_{\text{ext}} \cdot d\mathbf{A} + \int_D \mathbf{S}_s \cdot d\mathbf{A}. \quad (7)$$

This equation will be considered term by term. The first term is the power incident on the detector in the absence of a scatterer, W_i:

$$W_i = \int_D \mathbf{S}_i \cdot d\mathbf{A} = S_i D. \quad (8)$$

The second term in Eq. (7) is the contribution from mixing between the incident and scattered fields. This mixing term contributes to the extinguished power W_{ext} only near the forward-scattering direction. At other angles, the integrand $\mathbf{S}_{\text{ext}} \cdot d\mathbf{A}$ oscillates rapidly, providing no net contribution to the integral. This is the well-known optical theorem.[23] In practical far-field cases, the integral of this extinction term over the detector area is equivalent to the total extinguished power[19,20]:

$$\int_D \mathbf{S}_{\text{ext}} \cdot d\mathbf{A} \approx \int_\sigma \mathbf{S}_{\text{ext}} \cdot d\mathbf{A} = -W_{\text{ext}}. \quad (9)$$

The last term in Eq. (7) is the scattered power into the detector. When the solid angle subtended by the detector is small ($D \ll \sigma$), very little of the total scattered power is collected by the detector, and this contribution to the total detected power can therefore be neglected.

If the detector is large enough to fully intercept the incident beam, the resulting expression for the detected power is

$$W_d \approx W_i - W_{\text{ext}}. \quad (10)$$

As expected, the power detected is the incident power less the extinguished power.

B. Dipole Scatterer ($ka \ll 1$)

In this subsection, the special case of a dipole scatterer is discussed. The dipole model is strictly valid for isolated particles of radius $a \ll 1/k$. This is valid in the near, intermediate, and far fields of the particle. For a justification of this approximation, see, for example, the book by Bohren and Huffman.[20] The electric field consists of the incident optical fields $\mathbf{E}_i$ and $\mathbf{H}_i$ and the dipole scattering terms $\mathbf{E}_s$ and $\mathbf{H}_s$. To obtain an expression for the extinguished power, we integrate the extinction component of the Poynting vector over the detector surface (or the optical theorem is used). To obtain an expression for the scattered power, we integrate the Poynting vector over the entire surface σ. The absorbed power is then calculated as the difference between the extinguished power and the scattered power. The expressions for each of these, derived by Bohren and Huffman[20] are

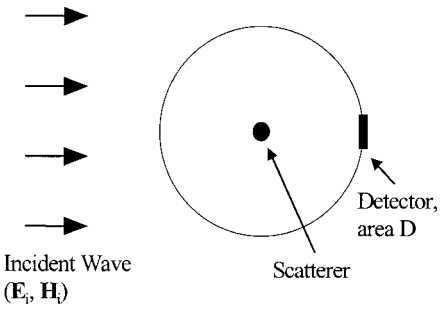

Fig. 4. Detector placed in the forward-scattering direction.

$$W_{\text{ext}} = \frac{1}{2}\epsilon_0 c {E_0}^2 \left[k\,\text{Im}(\alpha) + \frac{k^4|\alpha|^2}{6\pi} \right],$$

$$W_{\text{abs}} = \frac{1}{2}\epsilon_0 c {E_0}^2 k\,\text{Im}(\alpha),$$

$$W_{\text{sca}} = \frac{1}{2}\epsilon_0 c {E_0}^2 \frac{k^4|\alpha|^2}{6\pi}, \quad (11)$$

where α is the dipole polarizability and the field-induced dipole moment p is given by $p = \epsilon_0 \alpha E_0$.

This is an important result. To first order, only the imaginary component of the polarizability (absorption) is measured in far-field extinction measurements. In contrast, we will see in Section 3 that to first order in near-field photodetection measurements, the real part of the polarizability is measured. Note that if coherent illumination is used, the real component of the polarizability could be accessed in the far field by mixing the scattered beam with a reference beam with adjustable phase. Such a far-field measurement would be similar to the approach used in near-field scanning interferometric apertureless microscopy measurements.[3]

C. Spectroscopic Response in Absorption

In standard spectrophotometry, particles are seen to have a wavelength-dependent extinction cross section. If the spectral response of a dipole is modeled as a simple Lorentz oscillator of mass m, charge q, damping γ, and spring constant $k = m{\omega_0}^2$, then the oscillator's displacement x is governed by the following equation of motion:

$$\frac{q}{m} E_0 \exp(-i\omega t) - {\omega_0}^2 x - \gamma \dot{x} = \ddot{x}. \quad (12)$$

Solving this differential equation yields the Lorentzian response of the oscillator $x(\omega)$ and its dipole polarizability $\alpha(\omega)$ as follows:

$$x(\omega) = \frac{q/m}{{\omega_0}^2 - \omega^2 - i\omega\gamma} E_0 \exp(-i\omega t),$$

$$\alpha(\omega) = \frac{p}{\epsilon_0 E_0 \exp(-i\omega t)} = \frac{q^2/\epsilon_0 m}{{\omega_0}^2 - \omega^2 - i\omega\gamma} = \frac{\alpha_0 {\omega_0}^2}{{\omega_0}^2 - \omega^2 - i\omega\gamma},$$

$$\alpha_0 = \frac{q^2}{\epsilon_0 m {\omega_0}^2}. \tag{13}$$

These results will be used in the calculation of near-field power density in Subsection 3.C. Using these equations and the expression for extinction [the first of Eqs. (11)], the spectrally dependent extinguished power is

$$W_{\text{ext}} = \frac{1}{2}\epsilon_0 c {E_0}^2 \left[k \frac{\alpha_0 {\omega_0}^2 \omega\gamma}{({\omega_0}^2 - \omega^2)^2 + \omega^2\gamma^2} + \frac{k^4}{6\pi} \frac{{\alpha_0}^2 {\omega_0}^4}{({\omega_0}^2 - \omega^2)^2 + \omega^2\gamma^2} \right]. \tag{14}$$

The first term in the brackets is the contribution from $\text{Im}(\alpha)$, and the second term is the contribution from $|\alpha|^2$.

To summarize the far-field section, in conventional far-field spectrophotometry, extinction is measured. Extinction is the power removed from the incident beam by absorption and scattering. For a subwavelength particle, this extinction measurement is proportional to the imaginary part of the particle polarizability [the first of Eqs. (11)]. The frequency response of a Lorentz oscillator has been reviewed. Equation (14) predicts the extinction of a particle in a far-field measurement as a function of optical frequency.

3. PHOTODETECTION IN THE NEAR FIELD

In this section, the local electric fields near an illuminated particle and detector probe are calculated. Absorbed power by the local detector probe in the near field of the illuminated particle will be determined and contrasted with the far-field extinction relation found in Section 2. The near field of a particle is defined as a region where $kr \ll 1$, where r is the distance from the particle and k is the wave number of the illumination light. In a discussion of far-field measurements, it is convenient to talk about extinction, which is the total power removed from an incident beam by scattering and absorption. In near-field measurements, the extinction concept does not work well. The concept of absorption by a small particle is clear enough, but the power detected by a near-field photodetector is not just the incident power less some extinction introduced by the particle, as in the far-field case [relation (10)]. In fact, the power absorbed by a local detector probe near a particle can in certain cases be larger than the power detected without the particle present.

We now examine the optical fields near an illuminated subwavelength particle. The particle is represented as a dipole. The total electric and magnetic fields from an oscillating dipole moment $\mathbf{p}$ are as follows[24]:

$$\mathbf{E}(\omega, \mathbf{r}) = \frac{1}{4\pi\epsilon_0} \exp(i\mathbf{k}\cdot\mathbf{r} - i\omega t) \left\{ \frac{1}{r^3}[3\hat{r}(\hat{r}\cdot\mathbf{p}) - \mathbf{p}] - \frac{ik}{r^2}[3\hat{r}(\hat{r}\cdot\mathbf{p}) - \mathbf{p}] - \frac{k^2}{r}[\hat{r}\times(\hat{r}\times\mathbf{p})] \right\},$$

$$\mathbf{H}(\omega, \mathbf{r}) = -\frac{i\omega}{4\pi} \exp(i\mathbf{k}\cdot\mathbf{r} - i\omega t) \left(\frac{1}{r^2} - \frac{ik}{r} \right) \mathbf{p}\times\hat{r}. \tag{15}$$

In the far field ($kr \gg 1$), the $1/r$ terms dominate; these are the radiation terms. In the near field ($kr \ll 1$), the $1/r^3$ term is dominant. Only the electric field has a $1/r^3$ term, resulting in a greater energy density of the electric field than of the magnetic field in this region. The ratio of electric energy density to magnetic energy density of these near-field terms is

$$\frac{U_E(r)}{U_H(r)} = \frac{\epsilon_0 |E|^2}{\mu_0 |H|^2} \approx \frac{1}{k^2 r^2}. \tag{16}$$

As can be seen, very close to the particle ($kr \ll 1$), this ratio can be much greater than 1, in contrast to the energy density ratio for a plane wave, where the ratio is 1.

In far-field measurements, the extinction cross section can be considerably larger than the physical cross section (πa^2, where a is the radius) of a particle. This is significant for near-field measurements because a large extinction cross section causes "focusing" of the optical power in the near and intermediate fields. When the extinction cross section is larger than the physical cross section, optical fields near the particle are larger than the illumination field. With resonant metal particles, the ratio of extinction to physical cross section can be large. A 200-nm aluminum particle illuminated at an energy of 8.8 eV has an excited surface plasmon resonance. This resonance produces a large absorption, resulting in a ratio of extinction to physical cross section of 18. In this case, near the particle surface along the incident direction, the magnitude of the Poynting vector is more than 18 times larger than that of the incident illumination.[20]

A. Absorption by the Probe

In a near-field photodetection experiment, the photodetector is brought into the optical near field of an illuminated particle (see Fig. 5). Optical power is absorbed by the photodetector from the local fields. The sample particle and the detector probe are treated as optical dipoles. This is an approximation that keeps only the first-order term of a multipole expansion of the electromagnetic field. The advantage of this approximation is that it yields a simple model that aids in understanding the basic qualitative features of the experiment. Equations (11) include an expression for the power absorbed by a dipole of polarizability α under illumination. This expression can be obtained by calculating the average rate of work done on the dipole by the local electric field $\mathbf{E}$. The force $\mathbf{F}$ and the displacement $\mathbf{x}$ for the dipole that is due to the field are

$$\mathbf{F} = q\mathbf{E},$$

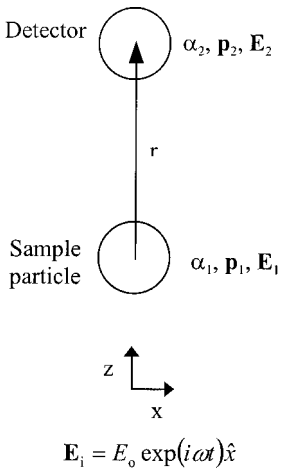

Fig. 5. Detector and sample particle illuminated in the near field. Both are modeled as dipoles. Here the detector is directly above the sample particle.

$$\mathbf{x} = \frac{\mathbf{p}}{q} = \frac{\epsilon_0 \alpha \mathbf{E}}{q},$$

$$\dot{\mathbf{x}} = -\frac{i\omega\epsilon_0\alpha\mathbf{E}}{q}. \tag{17}$$

The average rate of work done on the dipole is calculated to obtain the following absorbed power:

$$W = \frac{1}{2}\mathrm{Re}(\mathbf{F}\cdot\dot{\mathbf{x}}^*) = \frac{\epsilon_0 c|E|^2}{2} k\,\mathrm{Im}(\alpha), \tag{18}$$

where E is the amplitude of the local field seen by the detector.

B. Two Illuminated Dipoles in the Near Field

We now examine the interaction between the detector and the sample dipole (see Fig. 5). α_1, $\mathbf{p}_1$, and $\mathbf{E}_1$ are, respectively, the polarizability, the dipole moment, and the electric field seen by the sample particle (dipole 1). α_2, $\mathbf{p}_2$, and $\mathbf{E}_2$ are the corresponding quantities for the detector (dipole 2). This calculation must be performed self-consistently, since the field seen by one dipole depends upon the field seen by the other. Both particles see the incident field. Here the explicit time dependence is omitted, the phase delay between particles is assumed to be negligible, and only the largest near-field term of the dipole field is kept:

$$\mathbf{E}_1 = E_0\hat{x} + \frac{1}{4\pi\epsilon_0}\frac{1}{r^3}[3\hat{r}_{12}(\hat{r}_{12}\cdot\mathbf{p}_2) - \mathbf{p}_2],$$

$$\mathbf{E}_2 = E_0\hat{x} + \frac{1}{4\pi\epsilon_0}\frac{1}{r^3}[3\hat{r}_{21}(\hat{r}_{21}\cdot\mathbf{p}_1) - \mathbf{p}_1],$$

$$\mathbf{p}_1 = \alpha\epsilon_0\mathbf{E}_1,$$

$$\mathbf{p}_2 = \alpha\epsilon_0\mathbf{E}_2, \tag{19}$$

If one particle is directly above the other, as shown in Fig. 5, then

$$\mathbf{p}_1 = p_1\hat{x}, \quad \mathbf{p}_2 = p_2\hat{x}, \quad \hat{r}_{12} = -\hat{z}, \quad \hat{r}_{21} = \hat{z}, \tag{20}$$

$$E_1\hat{x} = \left(E_0 - \frac{\alpha_2 E_2}{4\pi r^3}\right)\hat{x}, \quad E_2\hat{x} = \left(E_0 - \frac{\alpha_1 E_1}{4\pi r^3}\right)\hat{x}, \tag{21}$$

$$E_1 + \frac{\alpha_2}{4\pi r^3}E_2 = E_0, \quad E_2 + \frac{\alpha_1}{4\pi r^3}E_1 = E_0. \tag{22}$$

Solving these two equations for E_1 and E_2 yields

$$E_1 = \frac{E_0\left(1 - \frac{\alpha_2}{4\pi r^3}\right)}{1 - \frac{\alpha_1\alpha_2}{16\pi^2 r^6}}, \quad E_2 = \frac{E_0\left(1 - \frac{\alpha_1}{4\pi r^3}\right)}{1 - \frac{\alpha_1\alpha_2}{16\pi^2 r^6}}. \tag{23}$$

E_2 is the electric field "seen" by the detector when directly above the sample particle ($\theta = 0$).

Now a specific physical example is given. A 5-nm-radius silicon probe (α_2) is brought into the near field of a 5-nm-diameter illuminated polystyrene particle (α_1) (see Fig. 6). The imaginary part of the relative permittivity of silicon is less than one tenth of the real part at 600 nm and will be neglected in calculation of the electric field. The field E_2 seen by the probe is

$$E_2 = E_0\frac{1 - \frac{\alpha_{\mathrm{polystyrene}}}{4\pi r^3}}{1 - \frac{\alpha_{\mathrm{polystyrene}}\alpha_{\mathrm{silicon}}}{16\pi^2 r^6}}. \tag{24}$$

The $1/r^6$ term in the denominator is of the order of 10^{-4} and will be neglected, yielding an error of 0.01%. For a spherical particle, the electrostatic polarizability is

$$\alpha = 4\pi\frac{\epsilon_r - 1}{\epsilon_r + 2}a^3, \tag{25}$$

where ϵ_r is the relative dielectric constant and a is the radius of the particle. The polarizabilities of the silicon detector probe and the polystyrene particle are

$$\frac{\alpha_{\mathrm{silicon}}}{4\pi} = 0.8a^3, \quad \frac{\alpha_{\mathrm{polystyrene}}}{4\pi} = 0.3a^3. \tag{26}$$

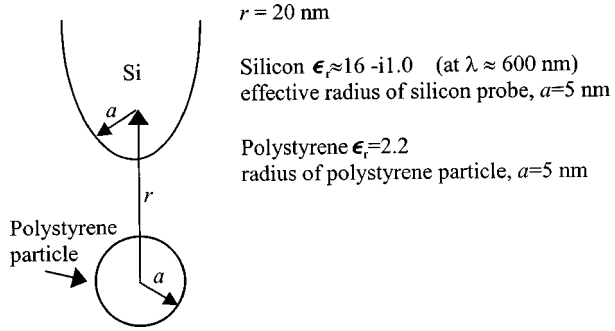

Fig. 6. Specific example of a polystyrene particle and a silicon probe.

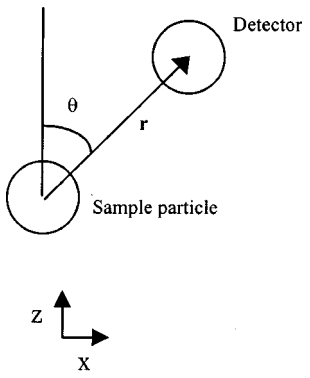

Fig. 7. The power absorbed by the detector for arbitrary r and θ is calculated.

The resultant electric field seen by the detector particle at a distance r of 20 nm is

$$E_2 \approx E_0[1 - 0.3(a/r)^3] = 0.995E_0. \tag{27}$$

Note that in this particular case, the field 20 nm above the particle is just 0.5% less with the particle than without the particle.

We will now consider other angles θ (see Fig. 7). Neglecting the terms of order α^2/r^6 or higher will greatly simplify the calculations with little effect on the accuracy ($\sim$0.01% error for the polystyrene example). The general expressions for the electric fields in this approximation are

$$\begin{aligned}\mathbf{E}_2 &\approx E_0\hat{x} + \frac{1}{4\pi\epsilon_0}\frac{1}{r^3}\{3\hat{r}_{21}[\hat{r}_{21} \cdot (\alpha_1\epsilon_0 E_0\hat{x})] \\ &\quad - (\alpha_1\epsilon_0 E_0\hat{x})\} \\ &\approx E_0\hat{x} + \frac{\alpha_1 E_0}{4\pi}\frac{1}{r^3}[3\hat{r}_{21}(\hat{r}_{21} \cdot \hat{x}) - \hat{x}],\end{aligned}$$

$$\begin{aligned}|\mathbf{E}_2|^2 &= {E_0}^2 + \frac{\mathrm{Re}(\alpha_1){E_0}^2}{2\pi}\frac{1}{r^3}[3(\hat{r} \cdot \hat{x})^2 - 1] \\ &\quad + \text{terms of order}\frac{|\alpha|^2}{r^6}.\end{aligned} \tag{28}$$

As shown in Eq. (18), the power absorbed by an illuminated detector dipole is proportional to the square of the electric field seen by the detector. In the present calculation, the power absorbed by the detector, W_2, is

$$W_2 = \tfrac{1}{2}\epsilon_0 c {E_2}^2 k\ \mathrm{Im}(\alpha_2). \tag{29}$$

with the equation for the field E_2 subtituted into Eq. (29), the power absorbed by the detector probe is shown below, where α_2 is the polarizability of the probe and α_1 is the polarizability of the sample particle:

$$\begin{aligned}W_2 &\approx \frac{1}{2}\epsilon_0 c k\ \mathrm{Im}(\alpha_2){E_0}^2 \\ &\quad \times\left[1 + \frac{\mathrm{Re}(\alpha_1)}{2\pi}\frac{1}{r^3}(3\sin^2\theta\cos^2\varphi - 1)\right].\end{aligned} \tag{30}$$

This expression is significant. It establishes that in near-field photodetection measurements, the real part of the polarizability of the sample particle is measured (to first order) in contrast to the far-field case, in which the imaginary part of the polarizability is the measured quantity (see Subsection 2.B). To a higher order, the square modulus of the polarizability, $|\alpha|^2$, is also measured in both. For a very small particle, the higher-order $|\alpha|^2$ term will be much smaller than the term proportional to α and may not be detectable.

Another way of looking at this is to consider the square of the field seen by the detector:

$$|\mathbf{E}|^2 = |\mathbf{E}_i + \mathbf{E}_s|^2 = |\mathbf{E}_i|^2 + 2\,\mathrm{Re}(\mathbf{E}_i \cdot \mathbf{E}_s{}^*) + |\mathbf{E}_s|^2, \tag{31}$$

where $\mathbf{E}_i$ is the incident field and $\mathbf{E}_s$ is the field generated by the sample dipole (scattered field). If $\mathbf{E}_i \gg \mathbf{E}_s$, then $2\,\mathrm{Re}(\mathbf{E}_i \cdot \mathbf{E}_s{}^*)$ (the mixing term) is much larger than $\mathbf{E}_s{}^2$. For the case of a polystyrene sphere of 5-nm radius, the scattered field is 200 times smaller than the incident field. Therefore the mixing term, which has a linear dependence on polarizability, dominates the scattering term. (Note that these calculations are made for coherent light. Because the detector and the particle are so close together, any practical illumination source will satisfy the coherence condition required for these calculations and $\mathbf{E}_i$ and $\mathbf{E}_s$ will coherently interfere at the near-field detector.)

C. Spatial Power Distribution near a Particle

We now consider what the probe will detect as it is scanned laterally in x above the particle for various illumination frequencies ω (see Fig. 8). If the sample dipole is treated as a simple Lorentz oscillator, the real part of the polarizability, $\mathrm{Re}(\alpha)$, is

$$\mathrm{Re}[\alpha(w)] = \frac{\alpha_0{\omega_0}^2({\omega_0}^2 - \omega^2)}{({\omega_0}^2 - \omega^2)^2 + \omega^2\gamma^2}. \tag{32}$$

Considering only values of $\gamma \ll \omega_0$, far below resonance ($\omega \ll \omega_0$), we have

$$\mathrm{Re}(\alpha) \approx \alpha_0. \tag{33}$$

On resonance ($\omega = \omega_0$), the result is

$$\mathrm{Re}(\alpha) = 0. \tag{34}$$

Note that when $\mathrm{Re}(\alpha) = 0$, terms in α^2/r^6, which have been neglected so far in this analysis, become significant on resonance, giving

$$|\mathbf{E}|^2 = {E_0}^2\left[1 + O\left(\frac{\alpha^2}{r^6}\right)\right]. \tag{35}$$

Far above resonance ($\omega \gg \omega_0$), we find that

$$\mathrm{Re}(\alpha) \approx -\alpha_0\frac{{\omega_0}^2}{\omega^2}. \tag{36}$$

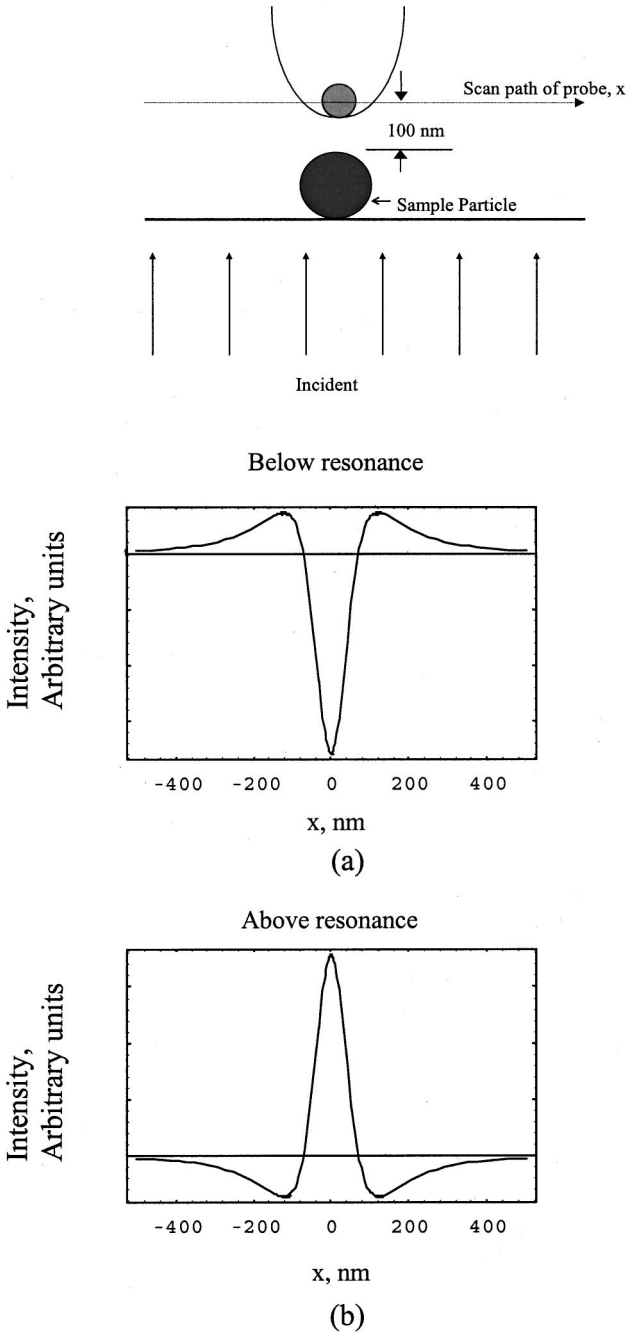

Fig. 8. The detector is scanned in the x direction above the sample particle. (a) The particle is illuminated below resonance. (b) The particle is illuminated above resonance.

In Fig. 8, E^2 is plotted as a function of position x with z = constant for an illumination frequency (a) far below resonance and (b) far above resonance. Note the contrast reversal that occurs between the below- and above-resonance cases. In Fig. 9, a plot of E^2 as a function of position x is shown for two sample dipoles separated by 200 nm. As indicated by the results shown in Fig. 9, near-field photodetection imaging should be capable of spatially resolving surface features that are separated by subwavelength dimensions. In the near field, the spatial distribution of $|E|^2$ is dependent on the dipole separation, not the illumination wavelength.

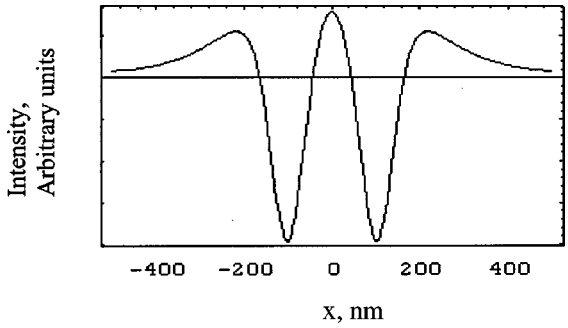

Fig. 9. Two particles, one at $x = 100$ nm and one at $x = -100$ nm, illuminated below resonance. The detector is scanned in the x direction above two sample particles separated by 200 nm.

4. INTERMEDIATE FIELD

In some local probe experiments, the probe is in the intermediate field of a sample particle ($kr \approx 1$). In this case, all three terms in Eq. (15) need to be included. In the intermediate field, the incident and scattered electric fields are

$$\mathbf{E}_i = E_0 \exp[ik(z - \omega t)]\hat{x},$$

$$\mathbf{E}_s = \frac{1}{4\pi\epsilon_0}\exp[ik(r - wt)]\left\{\frac{1}{r^2}[3\hat{r}(\hat{r}\cdot\mathbf{p}) - \mathbf{p}] - \frac{ik}{r^2}[3\hat{r}(\hat{r}\cdot\mathbf{p}) - \mathbf{p}] - \frac{k^2}{r}[\hat{r}\times(\hat{r}\times\mathbf{p})]\right\},$$

$$\mathbf{p} = \epsilon_{0\alpha}\alpha E_0\hat{x}. \tag{37}$$

The total field squared, as before, is

$$|E_{\text{tot}}|^2 = |E_i|^2 + 2\,\text{Re}(\mathbf{E}_i\cdot\mathbf{E}_s{}^*) + |E_s|^2. \tag{38}$$

Because the illumination is a plane wave, the first term, $|E_i|^2$, is a constant. The last term, $|E_s|^2$, is small for weak scattering and will be neglected. (As before, all terms of order $|\alpha|^2$ and higher are neglected.) The cross term, which provides the spatial contrast, is given by

$$\begin{aligned}
&2\,\text{Re}(\mathbf{E}_i\cdot\mathbf{E}_s{}^*)\\
&= \text{Re}\left(\frac{|E_0|^2\alpha^*}{2\pi}\exp[ik(z-r)]\left\{\frac{1}{r^3}[3(\hat{r}\cdot\hat{x})^2-1] + \frac{ik}{r^2}[3(\hat{r}\cdot\hat{x})^2-1] - \frac{k^2}{r}[(\hat{r}\cdot\hat{x})^2-1]\right\}\right)\\
&= \frac{|E_0|^2}{2\pi}\text{Re}(\alpha)\left\{\cos[k(z-r)]\left[-\frac{1}{r^3}\left(1-\frac{3x^2}{r^2}\right) + \frac{k^2}{r}\left(1-\frac{x^2}{r^2}\right)\right] + \sin[k(z-r)]\times\left[\frac{k}{r^2}\left(1-\frac{3x^2}{r^2}\right)\right]\right\} - \frac{|E_0|^2}{2\pi}\text{Im}(\alpha)\left\{\cos[k(z-r)]\times\left[\frac{k}{r^2}\left(1-\frac{3x^2}{r^2}\right)\right] - \sin[k(z-r)]\times\left[-\frac{1}{r^3}\left(1-\frac{3x^2}{r^2}\right) + \frac{k^2}{r}\left(1-\frac{x^2}{r^2}\right)\right]\right.
\end{aligned} \tag{39}$$

Recently developed experimental capabilities allow photodetection measurements to be performed in the near field.[12–14] We now describe one of these measurements and compare the measured result with our intermediate dipole model shown in Eq. (39). A 300-nm polystyrene sphere is illuminated with 536-nm light. The polarizability of the polystyrene sphere is dominantly real at this wavelength (well below the absorption resonance) with an index of refraction of 1.5. A silicon probe is scanned in the x direction at a constant height, as shown in Fig. 10(a). When the probe passes over the sphere, it is 100 nm above the sphere. If the sphere is approximated as a dipole positioned at the center of the sphere, the distance from the dipole to the probe is of order $1/k$; this places the probe in the intermediate field of this dipole. The calculated intensity versus x is shown in Fig. 10(b).

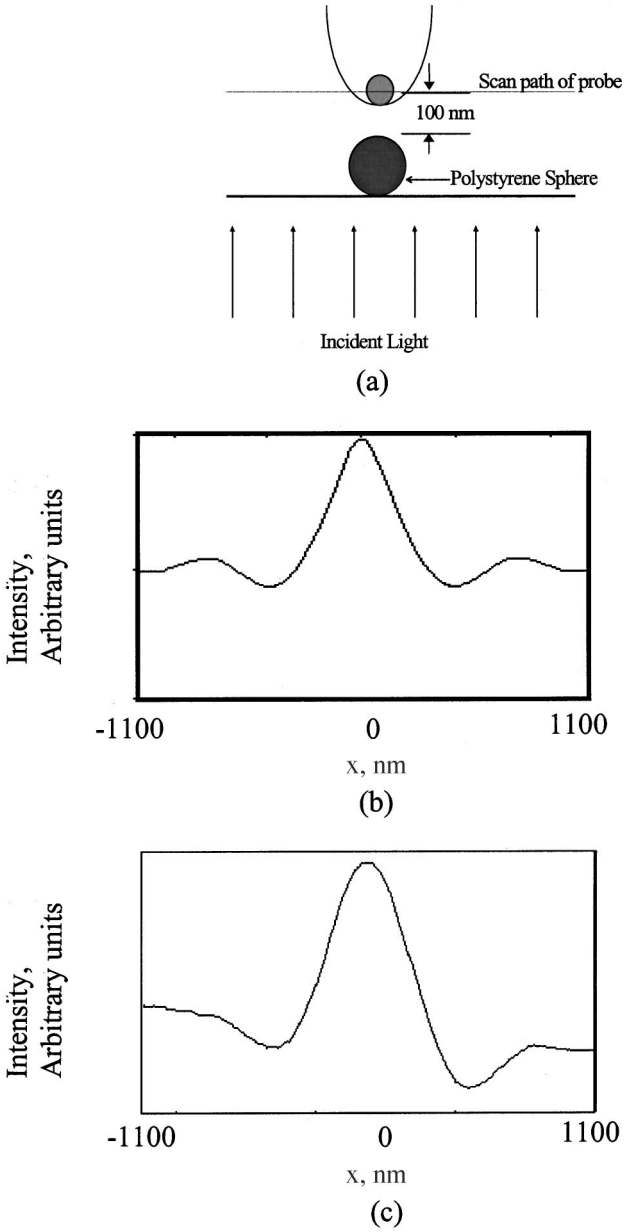

Fig. 10. Probe in the intermediate field. (a) The probe is scanned at a constant height above the particle. (b) Calculated intensity profile for the scan path shown in (a). In this calculation the probe is in the intermediate field of the sample particle. (c) Experimentally measured photocurrent in good agreement with the calculated linescan.

Note that the power absorbed by the probe is a maximum directly above the particle (for this intermediate-field case, below resonance). This result is opposite that of the near-field, below-resonance case [see Fig. 8(a)], where the response of the probe above the particle is a minimum. Also note the small oscillations of the probe response as the probe is moved laterally away from the particle, again in contrast with the near-field case. In Fig. 10(c), a measured near-field photodetection response as a function of lateral position is shown. This is in good qualitative agreement between the measured and predicted intermediate photodetection responses.

5. SUMMARY

In the near field of an illuminated sample particle, the electric field is dominantly $1/r^3$ dependent. This term is evanescent, as it decays rapidly in the far field. A small dipole probe, brought into the near field of a sample particle, absorbs power proportional to the local electric field amplitude squared. To first order, near-field photodetection directly measures the real part of the polarizability of the sample dipole. This is in contrast to far-field absorption measurements, which measure the imaginary part of the polarizability to first order. The near-field calculations also indicate that subwavelength features should be resolvable by near-field photodetection. Additionally, near a particle resonance there is a contrast reversal that occurs when the illumination frequency is changed from below resonance to above the particle resonance.

In the intermediate field, the spatial distribution of the intensity is qualitatively different from the near-field distribution. The most striking difference is a contrast reversal. For below-resonance illumination and in the near field, the detected power is a minimum directly above the particle. When the detector probe is likewise scanned in the intermediate field, the power detected has a maximum directly above the particle. This simple modeling indicates that photodetection measurement in the near and intermediate fields can provide unique optical information about the optical properties of small particles with subwavelength spatial resolution.

Address correspondence to R. C. Davis, Brigham Young University, Department of Physics and Astronomy, N215 ESC, P.O. Box 4644, Provo, Utah 84602-4644, or by e-mail, davis@byu.edu.

REFERENCES

1. E. Betzig and J. K. Trautman, "Near-field optics. Microscopy, spectroscopy, and surface modification beyond the diffraction limit," Science **257**, 189–195 (1992).
2. H. Heinzelmann and D. W. Pohl, "Scanning near-field optical microscopy," Appl. Phys. A: Solids Surf. **59**, 89–107 (1994).
3. F. Zenhausen, Y. Martin, and H. K. Wickramasinghe, "Scanning interferometric apertureless microscopy: optical imaging at 10 angstrom resolution," Science **269**, 1083–1085 (1995).

4. E. J. Sánchez, L. Novotny, and X. Sunney Xie, "Near-field fluorescence microscopy based on two-photon excitation with metal tips," Phys. Rev. Lett. **82**, 4014–4017 (1999).
5. D. R. Busath, R. C. Davis, and C. C. Williams, "Near-field photodetection optical microscopy (NPOM): a novel probe for optical characterization on a subwavelength spatial scale," in *Scanning Probe Microscopies II*, C. C. Williams, ed., Proc. SPIE **1855**, 75–85 (1993).
6. H. U. Danzebrink and U. C. Fischer, "The concept of an optoelectronic probe for near field microscopy," in *Near Field Optics*, D. W. Pohl and D. Courjon, eds. (Kluwer Academic, Dordrecht, The Netherlands, 1993), pp. 303–308.
7. D. R. Busath, "Near-field photodetection probe for near-field optical microscopy," Ph.D. thesis (University of Utah, Salt Lake City, Utah, 1994).
8. H.-U. Danzebrink, "Optoelectronic detector probes for scanning near-field optical microscopy," J. Microsc. (Oxford) **167**, 276–280 (1994).
9. R. C. Davis, C. C. Williams, and P. Neuzil, "Micromachined submicrometer photodiode for scanning probe microscopy," Appl. Phys. Lett. **66**, 2309–2311 (1995).
10. H.-U. Danzebrink, G. Wilkening, and O. Ohlsson, "Near-field optoelectronic detector probes based on standard scanning force cantilevers," Appl. Phys. Lett. **67**, 1981–1983 (1995).
11. S. Akamine, H. Kuwano, and H. Yamada, "Scanning near-field optical microscope using an atomic force microscope cantilever with integrated photodiode," Appl. Phys. Lett. **68**, 579–581 (1996).
12. R. C. Davis, C. C. Williams, and P. Neuzil, "Optical intensity mapping on the nanometer scale by near-field photodetection optical microscopy," Opt. Lett. **21**, 447–449 (1996).
13. R. C. Davis and C. C. Williams, "Nanometer-scale absorption spectroscopy by near-field photodetection optical microscopy," Appl. Phys. Lett. **69**, 1179–1181 (1996).
14. R. C. Davis, "Nanometer scale optical intensity mapping and absorption spectroscopy by near-field photodetection optical microscopy," Ph.D. dissertation (University of Utah, Salt Lake City, Utah, 1996).
15. C. Girard and D. Courjon, "Model for scanning tunneling optical microscopy: a microscopic self consistent approach," Phys. Rev. B **42**, 9340–9349 (1990).
16. D. Van Labeke and D. Barchiesi, "Theoretical problems in scanning near field optical microscopy," in *Near Field Optics*, D. W. Pohl and D. Courjon, eds. (Kluwer Academic, Dordrecht, The Netherlands, 1993), pp. 157–178.
17. L. Novotny, D. W. Pohl, and P. Regli, "Light propagation through nanometer-sized structures: the two-dimensional aperture scanning optical microscope," J. Opt. Soc. Am. A **11**, 1768–1779 (1994).
18. L. Novotny, "Allowed and forbidden light in near-field optics. II. Interacting dipolar particles," J. Opt. Soc. Am. A **14**, 105–113 (1997).
19. H. C. van de Hulst, *Light Scattering by Small Particles* (Dover, New York, 1981).
20. C. F. Bohren and D. R. Huffman, *Absorption and Scattering of Light by Small Particles* (Wiley, New York, 1983).
21. D. R. Pettit and T. W. Peterson, "Coherent detection of scattered light from submicron aerosols," Aerosol. Sci. Technol. **2**, 351–368 (1983).
22. D. R. Pettit, "Coherent extinction and self-homodyning by small particles," Appl. Opt. **26**, 5136–5142 (1987).
23. R. G. Newton, "Optical theorem and beyond," Am. J. Phys. **44**, 639–642 (1976).
24. J. D. Jackson, *Classical Electrodynamics*, 3rd ed. (Wiley, New York, 1998).